Current density in generalized Fibonacci superlattices under a uniform electric field

2008 J. Phys.: Condens. Matter 20 275243

(http://iopscience.iop.org/0953-8984/20/27/275243)

J. Phys.: Condens. Matter **20** (2008) 275243 (7pp) doi:10.1088/0953-8984/20/27/275243

Current density in generalized Fibonacci superlattices under a uniform electric field

P Panchadhyayee[1,2,4], R Biswas[1], Arif Khan[3] and P K Mahapatra[2]

[1] Prabhat Kumar College, Contai, Purba Medinipur, WB 721401, India
[2] Department of Physics and Technophysics, Vidyasagar University, Midnapore 721102, India
[3] Electrocom Corporation, PO Box: 60317, Potomac, MD 20859, USA

E-mail: ppcontai@gmail.com

Received 16 February 2008, in final form 18 April 2008
Published 13 June 2008
Online at stacks.iop.org/JPhysCM/20/275243

Abstract

We present an exhaustive study on tunneling and electrical conduction in an electrically biased GaAs–$Al_yGa_{1-y}As$ generalized Fibonacci superlattice. The study is based on transfer matrix formalism using an Airy function approach and provides an exact calculation of the current density in the case of quasi-periodic multibarrier systems. The results suggest the use of such quasi-periodic systems in perfect band-pass or band-eliminator (of extremely low width) circuitry. We have clearly demonstrated the resonance-type peaks and negative differential conductivity regimes in such systems. It has also been found that quasi-periodicity favors sharp negative differential conductivity peaks compared to those in periodic superlattices and thus have profound importance in device applications.

(Some figures in this article are in colour only in the electronic version)

1. Introduction

Semiconductor superlattices (SLs) have been a subject of great interest during the last two decades both from the fundamental point of view as well as for their potential device applications [1]. In particular, since the experimental realization of quasi-periodic SLs, such as Fibonacci [2] and Thue-Morse [3] SLs, the topic has gained momentum from experimental [4–6] and theoretical [7–15] viewpoints in the understanding of their unique physical properties, such as their electronic and transport properties. One of the most appealing motivations for these studies is the theoretical prediction that ideal quasi-periodic SLs should exhibit a highly fragmented electronic spectrum displaying self-similar patterns [16, 17].

To bring forth the motivation behind our proposed study adequately, it is worthwhile reviewing the salient features of electrical conduction in periodic SLs (PSLs) and the tunneling in semiconductor multibarrier systems (MBS). In an unbiased MBS the transmission coefficient shows resonant tunneling peaks at certain incident electron energies. These quasi-resonant tunneling energy states correspond to unit transmission coefficient and group themselves to band like clusters akin to mini energy bands in the PSLs [18]. In the PSLs the wavefunctions in the absence of electric field are extended in nature. When a uniform electric field is applied perpendicular to the growth axis, the electronic wavefunctions become localized (Wannier–Stark states) and the mini energy band passes into an equally spaced, discrete ladder-like spectrum (Wannier–Stark ladder). As a consequence of such localization the tunneling probability across the MBS decreases abruptly resulting in negative differential conductivity (NDC) regimes in the current–voltage characteristics. The NDC in dc-biased SL results in traveling electrical domain formation that may be used in a microwave source [19]. The NDC regions appear to be important for the quasi-periodic systems as these systems represent intermediate cases between periodic and disordered systems. Hence it is plausible to study the tunneling of electrons in electrically MBS and the electrical conduction in these quasi-periodic systems. The present study might help the experimentalists to fabricate the electronic devices by finding the NDC regimes in the current–voltage characteristics.

In some previously reported theoretical studies [13–15] on electrically biased Fibonacci superlattices (FSLs), the electrical conduction was studied by calculating Landauer resistance [15]. Here Landauer resistance was calculated by

[4] Address for correspondence: Department of Physics, Prabhat Kumar College, Contai, PO Contai, District Purba Medinipur, West Bengal, Pin-721401, India.

the transmission and reflection probabilities and is valid at zero temperature. But prior to device applications at room temperature, the knowledge of net tunneling current is very important as electrons with all possible energies contribute in the electrical conduction. Most of these works on Landauer resistance were based on an envelope function approach. No work has so far been reported on electrical conduction in the biased FSLs through the exact studies of current density and tunneling using Airy functions. For the case of electrically biased MBS, the transfer matrix method using the solution of Schrödinger's equation via Airy functions is treated as the most accurate method [20] of computing the transmission coefficient and then the current density. The current density calculated in the present approach [21] seems to be more realistic for device applications. The major problem dealing with Airy functions pertains to the numerical overflow of the Airy functions at low bias condition [22]. To overcome this problem, previous workers [13–15] have resorted to the asymptotic forms of the Airy functions, which compromises the accuracy of the result. But we have recently presented exact studies [23] on electrical conduction and tunneling in case of PSL under a uniform electric field using Airy functions, which take care of the problem of numerical overflow at low bias.

In view of the above discussion, we have presented the study on resonant tunneling in electrically biased GaAs–$Al_yGa_{1-y}As$ generalized Fibonacci-type superlattices (GFSL) [24] generated using a generalized Fibonacci sequence (GFS). In the first approximation, the SLs constructed by growing alternate layers of two semiconducting materials having similar band structures but with different energy gaps can be considered as quasi-1D systems of rectangular potential wells separated by barriers in the conduction band profile. Although this restriction may, at first sight, appear as a restrictive one, it turns out that many interesting properties of the SLs and polymer systems [25–27] can be properly described in terms of effective 1D Hamiltonians under reasonable conditions. The theoretical development is based on the transfer matrix approach using exact Airy function formalism and effective mass dependent boundary conditions [28]. Within this scheme, the main focus of our work is to calculate the exact current density directly from the transmission coefficient for these quasi-periodic systems.

The work is organized as follows. In section 2, we have detailed the theoretical scheme used for the transmission coefficient and the current density. Section 3 deals with the numerical analysis. Our multifarious results are discussed in section 4. Finally, our conclusions are presented in section 5.

2. Theoretical framework

The GFSLs can be generated by an iterative process according to the following rule: $S_{t+1} = [n[S_t]] \cdot [m[S_{t-1}]]$ where n and m are natural numbers; the index t defines the so-called generation number of GFS, $[n[S_t]]$ and $[m[S_{t-1}]]$ are meant for n and m repetitions of $[S_t]$ and $[S_{t-1}]$ respectively and '$\cdot$' denotes concatenation of strings. Table 1 presents a few initial generations of GFSs of two different kinds i.e., for the first case: $n = 1$, $m = 1 (S_{t+1})$ and another case: $n = 2$, $m = 1$ (S'_{t+1}). Here we have started the construction of GFS with $S_1 = S'_1 = A$, $S_2 = S'_2 = B$, where A and B are the elementary blocks made of a small gap material GaAs quantum well of width 'a' and of a large gap material $Al_yGa_{1-y}As$ barrier of thickness 'b' respectively. These two materials like GaAs and $Al_yGa_{1-y}As$ have similar band structures but different energy gaps. From the above table it is understood that quasi-periodicity increases more for S'_{t+1} than S_{t+1} [15]. Our model consists of total N barriers where barrier width is varied for different GFSs according to table 1.

Table 1. A few initial GFSs for different values of n and m.

t	S_{t+1}	$S_{t+1} = (S_t)^1 \cdot (S_{t-1})^1$	S'_{t+1}	$S'_{t+1} = (S_t)^2 \cdot (S_{t-1})^1$
1	S_1	A	S'_1	A
2	S_2	B	S'_2	B
3	S_3	BA	S'_3	BBA
4	S_4	BAB	S'_4	BBABBAB
5	S_5	BABBA	S'_5	BBABBABBBABBABBBA
6	S_6	BABBABAB		
7	S_7	BABBABABBABBA		

2.1. Transmission coefficient

In the SL, as the semiconductor layers come into contact, a discontinuity in the conduction band edge appears, which is equal to the difference in the chemical affinities of the materials. Further, the electrons have a tendency to spill over from the barrier layer to the wells on either side until the Fermi levels line up. Thus the charge transfer is expected to produce a symmetrical sagging on the roof of the rectangular barriers. For these semiconducting materials, the carrier concentration is of the order of 10^{16} cm^{-3}. In case of the SLs considered here, the barrier width is much less than 100 Å and the sagging produced in the rectangular shape of the barrier can be shown to be negligibly small in comparison to the barrier height [29]. Moreover, in such systems, as the screening length (ξ) is sufficiently large, the screening effect on the potential appearing through a multiplying factor ($e^{-x/\xi}$) is minimal. Hence for the calculation of the transmission coefficient we assume that the interfaces between the layers are sharply defined and devoid of any surface effects, so that the potential distribution may be considered to be an array of rectangular wells and barriers with the barrier height V_0.

The additional term in the Hamiltonian for a dc-biased SL can be obtained by solving the characteristic Poisson's equation which involves the dielectric constants of the materials. However, as the free carrier density is sufficiently small for the semiconductor SLs the external electric potential does not change significantly [15] in the well and barrier layers. Hence the potential representing the electrical bias is assumed to take the linear form $(-eEx)$ in both the barrier and the well regions. The schematic model of the conduction band of a one-dimensional GFSL in the presence of a uniform electric field E as shown in figure 1, is given as:

$$V(x) = \begin{cases} (V_0 - eEx) & \text{for } x_{nL} \leqslant x \leqslant x_{nR} \\ -eEx, & \text{otherwise,} \end{cases} \qquad (2.1.1)$$

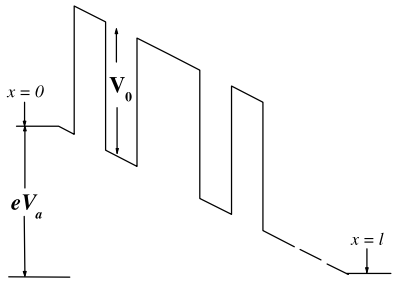

Figure 1. Potential energy profile for an electrically biased Fibonacci superlattice.

where x_{nL} and x_{nR} are the positions of the left and the right walls of the nth barrier respectively.

Under the influence of the field applied across the GFSL, the one-dimensional Schrödinger's equation in the well and the barrier regions respectively appears as

$$-\frac{\hbar^2}{2m_1^*}\frac{\mathrm{d}^2\psi^{(1)}}{\mathrm{d}x^2} - eEx\psi^{(1)} = \varepsilon\psi^{(1)}, \tag{2.1.2}$$

$$-\frac{\hbar^2}{2m_2^*}\frac{\mathrm{d}^2\psi^{(2)}}{\mathrm{d}x^2} + (V_0 - eEx)\,\psi^{(2)} = \varepsilon\psi^{(2)}, \tag{2.1.3}$$

where m_1^* and m_2^* are the respective position dependent effective masses in the well and barrier regions and ε is the incident electron energy.

Using Airy functions the solutions of (2.1.2) and (2.1.3) in the nth well and the nth barrier regions are obtained respectively as:

$$\psi_n^{(1)}(x) = A_{2n-1}Ai(\chi) + B_{2n-1}Bi(\chi), \tag{2.1.4}$$

where $n = 1, \ldots, (N+1)$; $\chi = -\alpha_1 x - \lambda_1$, $\alpha_1^2 = \frac{2m_1^* eE}{\hbar^2}$ and $\lambda_1 = \frac{2m_1^*\varepsilon}{\hbar^2\alpha_1^2}$,

$$\psi_n^{(2)}(x) = A_{2n}Ai(\varphi) + B_{2n}Bi(\varphi), \tag{2.1.5}$$

where $n = 1, 2, \ldots, N$; $\phi = -\alpha_2 x + \lambda_2$, $\alpha_2^2 = \frac{2m_2^* eE}{\hbar^2}$ and $\lambda_2 = \frac{2m_2^*(V_0-\varepsilon)}{\hbar^2\alpha_1^2}$.

With the use of effective mass dependent boundary conditions [28] which conserve both the probability density and the current density associated with the wavefunctions at the boundary of the heterojunction, the transfer matrix that correlates the amplitudes of the wavefunction on the right of the nth barrier with that on the left of the nth barrier is given by

$$\begin{bmatrix} A_{2n+1} \\ B_{2n+1} \end{bmatrix} = [M_n]\begin{bmatrix} A_{2n-1} \\ B_{2n-1} \end{bmatrix}. \tag{2.1.6}$$

Here $[M_n]$ being the transfer matrix whose elements have the following forms:

$$(M_n)_{11} = \frac{1}{w^2}\begin{vmatrix} Ai(\phi_{2n}) & Bi(\chi_{2n}) \\ c^{-1}Ai'(\phi_{2n}) & Bi'(\chi_{2n}) \end{vmatrix} \times \begin{vmatrix} Ai(\chi_{2n-1}) & Bi(\phi_{2n-1}) \\ cAi'(\chi_{2n-1}) & Bi'(\phi_{2n-1}) \end{vmatrix} - \frac{1}{w^2}\begin{vmatrix} Bi(\phi_{2n}) & Bi(\chi_{2n}) \\ c^{-1}Bi'(\phi_{2n}) & Bi'(\chi_{2n}) \end{vmatrix} \times \begin{vmatrix} Ai(\chi_{2n-1}) & Ai(\phi_{2n-1}) \\ cAi'(\chi_{2n-1}) & Ai'(\phi_{2n-1}) \end{vmatrix}$$

$$(M_n)_{12} = \frac{1}{w^2}\begin{vmatrix} Ai(\phi_{2n}) & Bi(\chi_{2n}) \\ c^{-1}Ai'(\phi_{2n}) & Bi'(\chi_{2n}) \end{vmatrix} \times \begin{vmatrix} Bi(\chi_{2n-1}) & Bi(\phi_{2n-1}) \\ cBi'(\chi_{2n-1}) & Bi'(\phi_{2n-1}) \end{vmatrix} - \frac{1}{w^2}\begin{vmatrix} Bi(\phi_{2n}) & Bi(\chi_{2n}) \\ c^{-1}Bi'(\phi_{2n}) & Bi'(\chi_{2n}) \end{vmatrix} \times \begin{vmatrix} Bi(\chi_{2n-1}) & Ai(\phi_{2n-1}) \\ cBi'(\chi_{2n-1}) & Ai'(\phi_{2n-1}) \end{vmatrix}$$

$$(M_n)_{21} = -\frac{1}{w^2}\begin{vmatrix} Ai(\phi_{2n}) & Ai(\chi_{2n}) \\ c^{-1}Ai'(\phi_{2n}) & Ai'(\chi_{2n}) \end{vmatrix} \times \begin{vmatrix} Ai(\chi_{2n-1}) & Bi(\phi_{2n-1}) \\ cAi'(\chi_{2n-1}) & Bi'(\phi_{2n-1}) \end{vmatrix} + \frac{1}{w^2}\begin{vmatrix} Bi(\phi_{2n}) & Ai(\chi_{2n}) \\ c^{-1}Bi'(\phi_{2n}) & Ai'(\chi_{2n}) \end{vmatrix} \times \begin{vmatrix} Ai(\chi_{2n-1}) & Ai(\phi_{2n-1}) \\ cAi'(\chi_{2n-1}) & Ai'(\phi_{2n-1}) \end{vmatrix}$$

$$(M_n)_{22} = -\frac{1}{w^2}\begin{vmatrix} Ai(\phi_{2n}) & Ai(\chi_{2n}) \\ c^{-1}Ai'(\phi_{2n}) & Ai'(\chi_{2n}) \end{vmatrix} \times \begin{vmatrix} Bi(\chi_{2n-1}) & Bi(\phi_{2n-1}) \\ cBi'(\chi_{2n-1}) & Bi'(\phi_{2n-1}) \end{vmatrix} + \frac{1}{w^2}\begin{vmatrix} Bi(\phi_{2n}) & Ai(\chi_{2n}) \\ c^{-1}Bi'(\phi_{2n}) & Ai'(\chi_{2n}) \end{vmatrix} \times \begin{vmatrix} Bi(\chi_{2n-1}) & Ai(\phi_{2n-1}) \\ cBi'(\chi_{2n-1}) & Ai'(\phi_{2n-1}) \end{vmatrix},$$

where $\chi_{2n-1} = -\alpha_1 x_{\mathrm{nL}} - \lambda_1$, $\varphi_{2n-1} = -\alpha_2 x_{\mathrm{nL}} + \lambda_2$, $\chi_{2n} = -\alpha_1 x_{\mathrm{nR}} - \lambda_1$, $\varphi_{2n} = -\alpha_2 x_{\mathrm{nR}} + \lambda_2$, $\frac{1}{c} = \frac{m_1^*\alpha_2}{m_2^*\alpha_1}$ and the Wronskian, $w = Ai(\chi_i)Bi'(\chi_i) - Bi(\chi_i)Ai'(\chi_i)$; i being any integer.

Let the field be applied between $x = 0$ and l; l being the total length of GFSL. The transfer matrices, designated by $[I]$ and $[O]$ correlate the amplitudes of the wave functions in the left and right sides of $x = 0$ and $x = l$, respectively. Finally the transfer matrix that correlates the amplitudes of the wavefunctions for $x < 0$ and $x > l$ takes the shape:

$$\begin{bmatrix} A_F \\ B_F \end{bmatrix} = [O]\prod_{n=1}^{N}[M_n][I]\begin{bmatrix} A_0 \\ B_0 \end{bmatrix} = [W_N]\begin{bmatrix} A_0 \\ B_0 \end{bmatrix}, \tag{2.1.7}$$

where

$$[O] = \frac{1}{2}\begin{bmatrix} (Ai(\chi_F) - \frac{\alpha_1}{\mathrm{i}k'}Ai'(\chi_F))\exp(-\mathrm{i}k'nd) & (Bi(\chi_F) - \frac{\alpha_1}{\mathrm{i}k'}Bi'(\chi_F))\exp(-\mathrm{i}k'nd) \\ (Ai(\chi_F) + \frac{\alpha_1}{\mathrm{i}k'}Ai'(\chi_F))\exp(\mathrm{i}k'nd) & (Bi(\chi_F) + \frac{\alpha_1}{\mathrm{i}k'}Bi'(\chi_F))\exp(\mathrm{i}k'nd) \end{bmatrix},$$

$$[I] = \frac{1}{w}\begin{bmatrix} Bi'(\chi_0) + \frac{\mathrm{i}k}{\alpha_1}Bi(\chi_0) & Bi'(\chi_0) - \frac{\mathrm{i}k}{\alpha_1}Bi(\chi_0) \\ -\left(Ai'(\chi_0) + \frac{\mathrm{i}k}{\alpha_1}Ai(\chi_0)\right) & -\left(Ai'(\chi_0) - \frac{\mathrm{i}k}{\alpha_1}Ai(\chi_0)\right) \end{bmatrix},$$

$$k^2 = \frac{2m_1^*\varepsilon}{\hbar^2} \qquad \text{and} \qquad k'^2 = \frac{2m_1^*}{\hbar^2}(\varepsilon + eEl).$$

Here $[W_N]$ refers to the transfer matrix that relates the coefficient matrix of the incoming and outgoing wave in the N barrier system. It has been found that the determinant of the transfer matrix $[W_N]$ is equal to unity.

As the outgoing wave has no reflection component, we can take $B_F = 0$. Using this fact, the transmission coefficient (τ_c) across N barriers can be given as [10, 13, 14, 23]

$$\tau_c = \frac{|A_F|^2}{|A_0|^2} = \left|\frac{\det[W_N]}{(W_N)_{22}}\right|^2. \tag{2.1.8}$$

2.2. Current density

The current density (J), calculated using τ_c from (2.1.8) for a one-dimensional system, is expressed as [21]

$$J = \frac{em^*k_BT}{2\pi^2\hbar^3}\int_0^\infty \left(\frac{k'}{k}\right)\tau_c \times \ln\left[\frac{1+\exp\{(E_F-\varepsilon)/k_BT\}}{1+\exp\{(E_F-\varepsilon-eV_a)/k_BT\}}\right] d\varepsilon, \tag{2.2.1}$$

where E_F is the Fermi energy, ε the incident energy, V_a the overall applied bias, T the absolute temperature.

3. Numerical analysis

We have calculated the transmission coefficient of the chosen GFSL in the below-barrier condition ($\varepsilon < V_0$) and also the current density for the applied uniform electric field in a wide range of model parameters. Since most of the practical devices are mainly concerned with applications at room temperature we have selected $T = 300$ K for most of our calculations. We have performed our calculations for a GaAs–$Al_{0.3}Ga_{0.7}As$ GFSL, assuming the conduction band discontinuity (V_0) = 370.1 meV [30] and electron effective masses, $m_1^* = 0.065\, m_0$, $m_2^* = 0.0919\, m_0$, where m_0 is the free electron mass. For a GaAs–$Al_{0.3}Ga_{0.7}As$ GFSL, we have taken $n = 1$, $m = 1$ (S_{t+1}) and $n = 2$, $m = 1$ (S'_{t+1}) for two initial types of GFS as in table 1. For convenience, we will simply refer to S_{t+1} as the first type GFSL and S'_{t+1} as the second type GFSL. The lattice constants for the well and barrier materials are considered as 5.6533 Å and 5.65564 Å respectively. The width 'a' of the well block of the low gap material is kept fixed by taking the number of unit cells (nwc) equals to 5. But the width 'b' of the barrier block of the high gap material consists of a variable number of unit cells (nbc = 1–5). For the study of tunneling in the presence of a uniform electric field, the values of applied field are chosen as 1, 10^5, 10^6 and 10^7 V m^{-1}. For an exactly zero field, the calculation based on the Airy function is not possible as the argument of the function contains the field parameter in the denominator. So for all practical purposes, the electric field of 1 V m^{-1} can be treated as the unbiased condition (field-free case). For the computational of J by (2.2.1), we select the value of Fermi energy as 0.069 eV at $T = 300$ K. Here the Fermi energy is taken as half the energy difference between the conduction band edge of the well material and the edge of the lowest miniband in the conduction band of the SL calculated on the basis of a model proposed earlier [31]. To show the temperature variation of current density the model parameters are also calculated accordingly for these systems at $T = 200$ K.

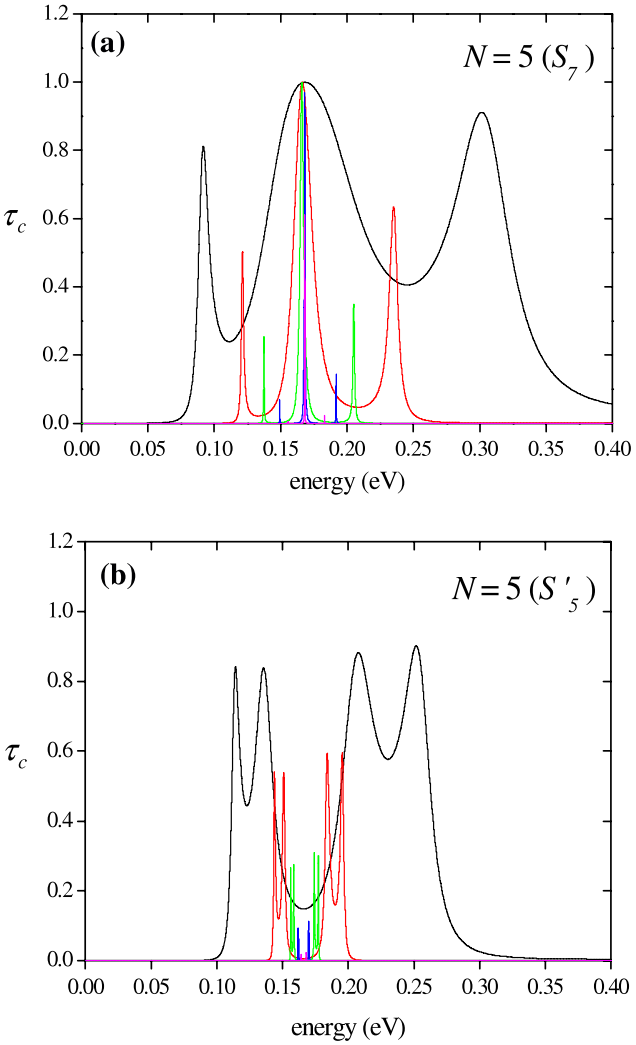

Figure 2. Variation of transmission coefficient (τ_c) versus incident electron energy (ε) (0–0.4 eV) for number of barrier cells, nbc = 1 (black online, (i) in the printed edition), 2 (red online, (ii) in the printed edition) 3 (green online, (iii) in the printed edition) 4 (blue online, (iv) in the printed edition) and 5 (magenta online, (v) in the printed edition) in the case of a total number of barriers, $N = 5$ for the unbiased (a) first type (S_7) GFSL (b) second type (S'_5) GFSL using the GaAs–$Al_{0.3}Ga_{0.7}As$ system.

4. Results and discussion

The transmission coefficient is numerically evaluated on the basis of (2.1.8) for five barriers in the first (S_7 generation) and second (S'_5 generation) types of GaAs–$Al_{0.3}Ga_{0.7}As$ GFSL. At first we have focused our attention on the resonance-type tunneling with the variation of barrier width for both the cases (figures 2(a) and (b)) to choose the appropriate nbc for which optimal resonant tunneling can occur. The transmission

coefficients for both the types in unbiased condition are plotted against incident energy (0–0.4 V) and shown in figures 2(a) and (b) respectively. From the tunneling point of view, it is important to study the transmittance in the below-barrier region. In the unbiased PSL the resonant tunneling corresponds to τ_c equal to unity across the structure and the incident energies at which the resonant tunneling occurs are termed as resonant tunneling energies. Any electron having energy equal to any one of these quasi-level resonant energies tunnels out across a SL without any significant attenuation in its intensity. Resonant tunneling is a consequence of the phase coherence of electron waves in the quantum wells of SL. The quasi-level resonant energies forming a band like cluster correspond to a miniband in the SL. The number of such states in each cluster for an N-barrier periodic MBS is found to be $(N-1)$ which is equal to the number of wells in the MBS. It is worth pointing out that a miniband in a PSL with N barriers contains $(N-1)$ energy levels. In the forbidden region τ_c remains almost zero. But we find some remarkable changes in the case of FSLs. In the below-barrier region for the first type GFSL (figure 2(a)), although there are four wells, we obtain almost three resonance-type tunneling peaks for all the different values of barrier width. In all these cases the central peak having the maximum τ_c occurs at a particular energy, $\varepsilon_c = 0.168$ eV which corresponds to the only resonant energy state of a periodic double barrier system [23]. The cluster of resonance-type energy states has been found to be symmetric around ε_c due to coupling of the wells. With an increase in the nbc value i.e., the barrier width, it is also observed that the other peaks decrease systematically and seem to move towards ε_c. This can be easily understood by the fact that the coupling among the wells decreases with an increase in barrier width and the transmittance spectrum finally tends to that of an isolated finite single well. To study the case of the second type GFSL also having four wells, we have obtained 4 tunneling peaks (figure 2(b)) for all nbc values in the region, $\varepsilon < V_0$. It is interesting to note that the 4 peaks for all values of nbc are evenly distributed around the same energy, $\varepsilon_c = 0.168$ eV. The height of all tunneling peaks diminishes systematically with increasing nbc like that of the first type GFSL. But the only exception is that the energy ε_c corresponds to a resonant tunneling level for the first type GFSL and a forbidden level for the second type. Figure 2(a) suggests that the first type GFSL for nbc $= 5$ can act as extremely low width (around ε_c) band-pass filter whereas the second type GFSL as a band-eliminator for the same nbc values (figure 2(b)) [12]. It is worth of mentioning that the distribution of 3 peaks (first type) and 4 peaks (second type) seems to be akin to the distribution of an odd and even number of energy states respectively around the central energy in a parabolic $\varepsilon - k$ diagram. As the main objective of figures 2(a) and (b) is concerned with finding the optimal resonant tunneling with respect to the heights of resonance-type peaks associated with small resonance widths, nbc $= 2$ is found to be suitable for further calculations of GFSL.

Next for the sake of understanding the field-effect on τ_c, we have presented our results on τ_c in the below-barrier region against incident electron energy (0–0.4 eV) in GaAs–$Al_{0.3}Ga_{0.7}As$ GFSL for $N = 5$ barriers (figure 3(a) for PSL, figure 3(b) for the first type GFSL and figure 3(c) for the second type GFSL) under the dc electric fields, $E = 1$, 10^5, 10^6 and 10^7 V m^{-1} respectively. It has been found that the effect of electric field on the transmission property becomes remarkable beyond the field $\sim 10^5$ V m^{-1}. With the application of fields, $E = 10^5$ and 10^6 V m^{-1}, the important feature is that the quasi-resonant tunneling energy levels are found to get Stark shifted towards the lower energies as in PSL [23]. From these figures, it is prominent that the electric field has a greater influence on the transmission spectrum for the GFSLs in comparison with PSL. In case of the GFSLs, for $E = 10^6$ V m^{-1}, τ_c increases abruptly at some resonant energies and also suffers a decrease at some other resonant energies. But, at such a field, the transmission probability decreases for all resonant energies in case of PSL [23]. For $E = 10^7$ V m^{-1}, we observe a strong reduction of transmission properties resulting in the disappearance of several transmission peaks in all cases, which can be explained on the basis of the occurrence of localized Wannier–Stark states. To explain the change of peak heights or the absence of resonance-type peaks it will be relevant to discuss the energy levels and the wavefunctions in an PSL in the presence of a field. In a field-free PSL the wavefunctions are extended in nature due to overlapping of the wavefunctions of the individual wells. This makes the resonant tunneling in the MBS a distinct possibility. For low applied fields, the energy spectrum of an PSL is expected to retain all its features except being Stark shifted. This phenomenon is also clearly observed in the quasi-tunneling energy bands of GFSL for fields up to 10^6 V m^{-1}. With an increase in field, owing to the tilting of the bands, the wavefunctions become more and more localized resulting in a decrease in the tunneling probability. As a result, the number of resonance-type peaks gradually decreases. But the increase in τ_c at such field is due to the coincidence of the energy states of two consecutive wells. For larger fields at which the existence condition ($eEd \geqslant \varepsilon_{bw}$, ε_{bw} being the width of the miniband and d, the SL periodicity) [31] for the occurrence of discrete WSL is fulfilled, the localization of the wavefunctions corresponding to WSL states appears. Hence there is no overlap of the wavefunctions of individual wells and the tunneling probability reduces drastically.

Finally the current densities for the first and second types of GFSL are calculated directly from the transmission coefficient using (2.1.8). The current densities (J) computed at two different temperatures ($T = 200$ and 300 K) for $N = 5$ barriers in case of aforesaid GFSLs' and PSL on the basis of (2.2.1) are plotted against the applied bias (V) (0–1.5 V) in figure 4. It is worthwhile considering the case of PSL for the effective comparison with quasi-periodic case. In all these systems the J–V characteristics show resonance-type curves with NDC regimes in between resonance-type J peaks. These J peaks for PSL corresponding to higher bias have higher values of J. But for the GFSLs there are no such regular variation. Further, the first resonance-type peak and the first NDC regime in the conductivity curves appears for fields which satisfy the existence condition [31] for the WSL states in a PSL having similar dimensions. In the presence of WSL states the electrical conduction is guided by the hopping processes between the WSL states via optical

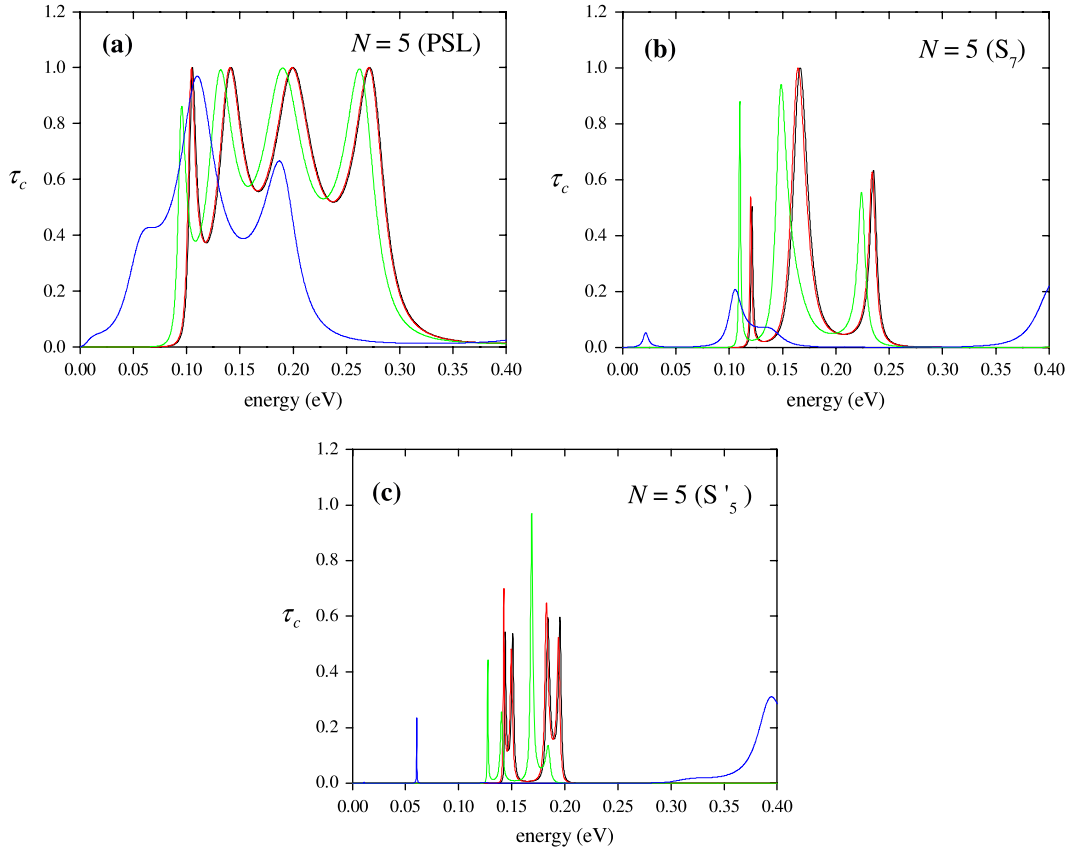

Figure 3. Variation of transmission coefficient (τ_c) versus incident electron energy (ε) (0–0.4 eV) for the (a) PSL, (b) first type (S_7) GFSL, (c) second type (S_5') GFSL using GaAs–$Al_{0.3}Ga_{0.7}As$ system in the case of total number of barriers, $N = 5$ with the electric field, $E = 1$ V m^{-1} (black online, (i) in the printed edition), 10^5 V m^{-1} (red online, (ii) in the printed edition), 10^6 V m^{-1} (green online, (iii) in the printed edition) and 10^7 V m^{-1} (blue online, (iv) in the printed edition).

phonon scattering. In the presence of WSL, the current–field relation exhibits resonant-type peaks in current for fields, $E_q = \hbar\omega/qed$, $q = 1, 2, \ldots$, etc, $\hbar\omega$ being the optical phonon energy. This feature corresponds to resonance-type transitions such that the phonon energy $\hbar\omega$ is an integral multiple of the spacing (eEd) of the WSL. Further, the increase in field increases the level spacing between WSL states causing a decrease in the hopping probability. The decrease of hopping probability with an increase in field brings a corresponding decrease in the current with an increase in the field and thereby establishes NDC. The phenomena also explain the appearance of resonance-type peaks and NDC regions in the current density curves for the quasi-periodic systems. It is further observed in figure 4 that the current density decreases with the increase in quasi-periodicity. This feature is more prominent in the low applied bias. Although the general nature of current density remains same, the sharpness of NDC regions increases and the corresponding peaks shift towards the low applied bias with the enhancement in quasi-periodicity, as seen for the cases of the first and second types of GFSL. Widths of NDC regions are also observed to be narrower as the degree of quasi-periodicity increases. This is due to the fractal character of electronic states of GFSL. Such a decrement in the width of the NDC regimes can be suitably exploited for device applications.

As far as the variation of temperature is concerned it is seen from figure 4 that there is an overall decrease in the current density with a lowering in temperature for all types of SL. This is due to the decrease in the number of thermally generated carriers in the system. The peaks of the current

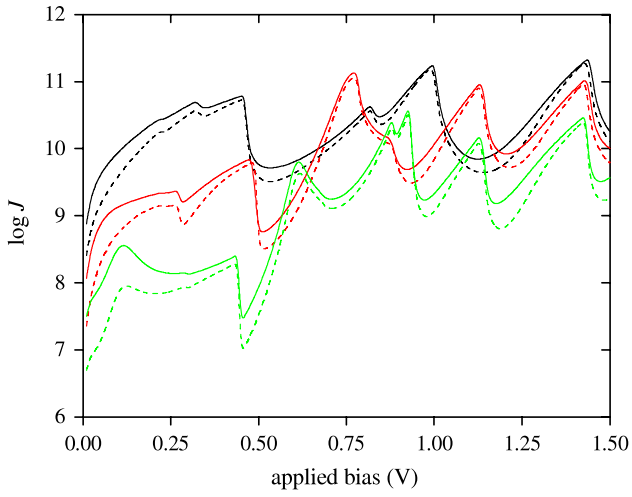

Figure 4. Current density (J)–voltage (V) characteristics for number of barriers, $N = 5$ in case of the PSL (black online, (a) in the printed edition), the first type (S_7) GFSL (red online, (b) in the printed edition) and the second type (S_5') GFSL (green online, (c) in the printed edition) using GaAs–$Al_{0.3}Ga_{0.7}As$ system at $T = 300$ K (solid line) and $T = 200$ K (broken line). Current density is given in A m^{-2}.

density curves show a tiny shift towards higher applied bias as the temperature is decreased. Although a little change is seen near the peaks, the temperature variation effect is significant near the troughs and thereby the NDC regions. From figure 4 it is well understood that the sharpness of the NDC regions increase with a decrease in temperature and the effect gets more pronounced with an increase in aperiodicity of the systems. A detailed study on the variation of J with T is under our active consideration.

5. Conclusion

In this paper we have presented the exact result on transmission coefficient and current density in case of two types of quasi-periodic GFSL under different electric fields. Like PSL, the transmittance spectrum for GFSL also exhibits resonance-type peaks and the corresponding resonant energy states group into bands separated by forbidden gaps. In the first type (S_7) GFSL, three resonance-type peaks are observed and they are distributed around the center of the band similar to the distribution of the odd number of states in an energy band. The central peak is found to be higher than the others. In the second type (S_5') GFSL, four resonance-type peaks are observed. The distribution of these transmission peaks in the band is similar to that of an even number of states in an energy band. Here the height of the peaks increases as we go from the center to the periphery of the tunneling band. Further, it is interesting to note that the electron with energy ε_c has the maximum tunneling probability for the first type GFSL but null tunneling probability for the second type GFSL. This phenomenon gives a clear indication for the use of GFSL as an effective electronic filter. The resonance-type peaks in both types of GFSL suffer Stark shift like PSL with the application of electric field. As expected for high fields in the case of PSL, the coupling between the quasi-resonant conduction energy levels becomes reduced and the incident electron waves get localized. Consequently, transmittance reduces significantly and the resonance-type peaks almost disappear. Though the same features are present in the case of both types of GFSL, the transmittance at some quasi-resonant energies, on the contrary, increases due to the coincidence of energy states in the two consecutive wells. Our results show that quasi-periodicity affects the current density significantly when compared with the situation in a periodic SL. The magnitude of current density decreases not only with an increase in aperiodicity but also with a decrease in temperature. Both aperiodicity and a lowering in temperature favor the comparatively sharp NDC characteristics which have a profound importance in the output power generation of the SL source, which depends on the current and voltage swing in the NDC region. Although the GaAs–$Al_yGa_{1-y}As$ GFSL has been used to test the applicability of the model, the features highlighted in this paper will be applicable in general for any system including GaN–$Al_yGa_{1-y}N$ which is a possible candidate for a high-power sub-millimeter wave source [32].

References

[1] Goossen K W, Cunningham J E and Jan W Y 1990 *Appl. Phys. Lett.* **57** 2582–4
[2] Merlin R, Bajema K, Clarke R, Juang F-Y and Bhattacharya P 1985 *Phys. Rev. Lett.* **55** 1768–70
[3] Merlin R, Bajema K, Nagle J and Ploog K 1987 *J. Physique Coll.* **48** C5 503–6
[4] Laruelle F, Etienne B, Barrau J, Khirouni K, Brabant J C, Amand T and Brousseau M 1990 *Surf. Sci.* **228** 92–5
[5] Munzar D, Bocaek L, Humlicek J and Ploog K 1994 *J. Phys.: Condens. Matter* **6** 4107–18
[6] Dinu M, Nolte D D and Melloch M R 1997 *Phys. Rev.* B **56** 1987–95
[7] Roy C L and Khan A 1994 *Phys. Rev.* B **49** 14979–83
[8] Roy C L, Khan A and Basu C 1995 *J. Phys.: Condens. Matter* **5** 1843–53
[9] Macia E, Dominguez-Adame F and Sanchez A 1994 *Phys. Rev.* B **49** 9503–10
[10] Dominguez-Adame F, Macia E, Mendez B, Roy C L and Khan A 1995 *Semicond. Sci. Technol.* **10** 797–802
[11] de Brito P E, da Silva C A A and Nazareno H N 1995 *Phys. Rev.* B **51** 6096–9
[12] Diez E, Dominguez-Adame F, Macia E and Sanchez A 1996 *Phys. Rev.* B **54** 16792–8
[13] Castro M and Dominguez-Adame F 1997 *Phys. Lett.* A **225** 321–5
[14] Reyes-Gómez E, Perdomo-Leiva C A, Oliveira L E and de Dios-Leyva M 1998 *J. Phys.: Condens. Matter* **10** 3557–67
[15] Tyc M H and Salejda W 2002 *Physica* A **303** 493–506
[16] Kohmoto M, Kadanoff L P and Tang C 1983 *Phys. Rev. Lett.* **50** 1870–2
[17] Ryu C S, Oh G Y and Lee M H 1993 *Phys. Rev.* B **48** 132–41
[18] Nanda J, Mahapatra P K and Roy C L 2006 *Physica* B **383** 232–42
[19] Schomburg E, Scheuerer R, Brandl S, Renk K F, Pavel'ev D G, Koschurinov Y, Ustinov V, Zhukov A and Kop'ev P S 1999 *Electron. Lett.* **35** 1491–2
[20] Gundlach K H 1966 *Solid-State Electron.* **9** 949–57
[21] Tsu R and Esaki L 1973 *Appl. Phys. Lett.* **22** 562–4
[22] Vatannia S and Gildenblat G 1996 *IEEE J. Quantum Electron.* **32** 1093–105
[23] Mahapatra P K, Panchadhyayee P, Bhattacharya S P and Khan A 2008 *Physica* B at press
[24] Gumbs G and Ali M K 1988 *Phys. Rev. Lett.* **60** 1081–4
[25] Maciá E and Domínguez-Adame F 2000 *Electrons, Phonons and Excitons in Low Dimensional Aperiodic Systems* (Madrid: Editorial Complutense)
[26] Albuquerque E L and Cottam M G 2003 *Phys. Rep.* **376** 225–337
[27] Maciá E 2006 *Rep. Prog. Phys.* **69** 397–441
[28] Bastard G 1981 *Phys. Rev.* B **24** 5693–7
[29] Mukherjee D and Nag B R 1975 *Phys. Rev.* B **12** 4338–45
[30] Mahapatra P K, Panchadhyayee P and Roy C L 2001 *Indian J. Pure Appl. Phys.* **39** 296–307
[31] Mahapatra P K, Bhattacharyya K, Khan A and Roy C L 1998 *Phys. Rev.* B **58** 1560–71
[32] Litvinov V I, Manasson A and Pavlidis D 2004 *Appl. Phys. Lett.* **85** 600–2